JOURNAL OF CATALYSIS 136, 170–181 (1992)

Reduction of Ni^{2+} Cations in Y Zeolites

II. Effect of the Environment

BRENDAN COUGHLAN AND MARK A. KEANE[1]

Physical Chemistry Laboratories, University College, Galway, Ireland

Received March 19, 1990; revised February 12, 1992

The reduction of Ni^{2+} cations supported on a range of both ion-exchanged and impregnated Y zeolites, enriched to various levels with Li^+, Na^+, K^+, Rb^+, Cs^+, NH_4^+, and Ce^{3+} cations, was investigated. The reduction process was found to be a dynamic equilibrium governed by the level of nickel exchange and the Brønsted acidity associated with each zeolite sample. At lower levels of exchange (<10 Ni^{2+}/UC), nickel reducibility is inversely related to the strength of coordination of the nickel ions to the zeolite lattice and increases in the order NiCsNaY < NiRbNaY < NiKY < NiNaY < NiLiY. At higher loadings, the percentage Ni^{2+} reduction decreases with increasing Brønsted acidity in the sequence NiCsNaY > NiRbNaY > NiKY > NiNaY> NiLiY. The reduction of Ni^{2+} ions supported on NH_4Y was negligible. In the case of the CeNiNaY and CeNiKY samples, the introduction of an additional level of acidity, due to the presence of the strongly polarizing Ce^{3+} ions during thermal activation served to further suppress the reduction process resulting in values of Ni^{2+} reduction lower than those of the NiNaY and NiKY samples. The effect of poisoning the acid sites by the adsorption of a number of bases was considered. Comparative data on the reduction of Ni^{2+} ions supported on alumina and silica are also included

INTRODUCTION

The role of the charge-balancing alkali metal co-cation in determining the nature and catalytic activity of the metal phase supported on Y zeolite has been the subject of a number of reports from this laboratory (*1–4*). In a previous paper (*5*), the effect of sample pretreatment on the degree of reduction of Ni^{2+} cations in the catalyst precursor was probed in some detail. Although the reduction of Ni^{2+} ions in faujasite zeolites has been studied extensively (*6–35*), the observed variety of phenomena associated with the mechanism and chemistry of the process is so confusing that the underlying principles need to be reconsidered. This paper is concerned with the influence of the zeolitic environment on the level of Ni^{2+} reduction and focuses on both monometallic nickel and nickel/cerium Y zeolites.

It has been deduced that an intercrystalline equilibrium exists between Ni^{2+} ions and reduced nickel, closely following the mass action law (*9, 11, 25, 26*),

$$(H_2)_g + Ni_z^{2+} \leftrightarrows 2\,H_z^+ + Ni_z^0,$$

where subscripts g and z represent the gas and zeolite phases, respectively. This implies that the reduction of nickel ions is retarded with increasing proton concentration, forcing the redox equilibrium to the left. The faujasite series does indeed show a decrease in reduced nickel with increasing acidity (*10, 11, 27*). Richardson (*10*) found that the reducibility of 3% (by weight) nickel faujasite decreased in the order NiNaY > NiLiY > NiCaY > NiMgNaY > $NiNH_4Y$ = 0. Exner *et al.* (*28*) have proposed a site-preferential reducibility that is related to the

[1] To whom correspondence should be addressed at Chemistry Department, Glasgow University, Glasgow G12 8QQ, Scotland.

0021-9517/92 $5.00

local acidity; i.e., the Ni^{2+} ions located in the hexagonal prisms are reduced preferentially in the presence of a high local proton activity in the supercages and sodalite cages.

The reducibility of a nickel ion exchanged into the zeolite lattice also depends on the presence of a second cation or metal in its environment. It has been established that the presence of trivalent cerium affects the location of Ni^{2+} ions in CeNiNaX zeolites (*18, 29*), on complete dehydration, S_I sites are preferentially occupied by Ce^{3+} ions, which essentially excludes the Ni^{2+} ions from the hexagonal prisms. Bager *et al.* (*17*) report that Ce^{3+} exchange decreases Ni^{2+} reducibility; whereas they found that Ca^{2+} (with a high S_I site selectivity) enhances metal formation. On the other hand, workers (*18, 19, 29–32*) at l'Universitaire Pierre et Marie Curie in Paris have carried out a series of studies that revealed a marked improvement in Ni^{2+} reduction on incorporating Ce^{3+} ions into NiNaX.

While impregnation with nickel nitrate has been extensively used in the preparation of nickel/alumina and nickel/silica catalysts, it has not been as widely applied to the preparation of nickel-loaded zeolites. To date, the majority of the documented studies on nickel-impregnated Zeolite Y (*26, 33–35*) have been from a catalytic viewpoint. Most of the factors that influence the reduction of nickel in zeolites also apply to the more traditional alumina and silica carriers. An increasing number of papers deal with new synthetic procedures designed to enhance the levels of Ni^{2+} reduction on such supports and these techniques have been reviewed by Marinas *et al.* (*36*). The percentage divalent nickel reduction decreases in the order (*10*) $Ni/SiO_2 > Ni–Al_2O_3/SiO_2 > Ni/Al_2O_3$. During the high-temperature treatment of Ni/Al_2O_3, NiO interacts with Al_2O_3 to form a very stable $NiAl_2O_4$ spinel which cannot be reduced even under extreme conditions (*37, 38*). Silica–alumina also complexes a small amount of nickel in a non-reducible form, whereas all the nickel supported on a silica carrier is reduced (*19*).

To date, there has been no systematic investigation into the consequences of varying the alkali metal co-cation or of the introduction of a rare earth (Ce^{3+}) cation on the level of reduction of Ni^{2+} supported on Y zeolites. Any co-cation-related effect will be of considerable importance in determining the nature of the catalytically active supported nickel species.

EXPERIMENTAL

The starting or parent zeolite was Linde molecular sieve LSZ-52, which can be represented by the molecular formula $Na_{58}(AlO_2)_{58}(SiO_2)_{134}(H_2O)_{260}$. The alumina (70–230 mesh) and silica (30–120 mesh) supports were supplied by Labkem Ltd. and BDH, respectively. The ion-exchange techniques used in this study have been described in detail elsewhere (*5*). The Li, K, Rb, Cs, and NH_4Y zeolites were prepared by refluxing the parent NaY with 0.5 mol dm^{-3} aqueous solutions of $LiNO_3$, KNO_3, RbCl, CsCl, and NH_4NO_3 over a period of 3 days, filtering and drying as before (*5*); after 10 such treatments, complete exchange was achieved. The nickel/cerium Y zeolites were prepared by first exchanging the NaY and KY supports with nickel cations. The dried zeolite was then refluxed with dilute solutions of $Ce(NO_3)_3$ to give a maximum exchange of ca. 4 Ce^{3+}/UC; for higher Ce^{3+} loadings, repeated exchange was necessary. Maximum cerium ion exchange of NaY and KY was reached at 68.0 and 74.2%, respectively. Quantitative impregnation of LiY, NaY, KY, RbNaY, CsNaY, NH_4Y, Al_2O_3, and SiO_2 was achieved with constant volumes of nickel nitrate solutions by vacuum rotary evaporation to incipient wetness. Each support was impregnated in a stepwise fashion with 0.1 mol dm^{-3} aqueous solutions of $Ni(NO_3)_2$ to yield the desired metal content. All the samples were air dried at 383 ± 3 K for 24 h and stored over saturated NH_4Cl solutions.

Thermal analyses were conducted on each sample using a Perkin–Elmer thermobalance operating in the TG and DTG modes to measure the water loss and rate of change of water loss, respectively, with temperature; the samples were heated at 40 K min^{-1} in the range 294–773 K under a 20 cm^3 min^{-1} nitrogen purge. The experimental procedures employed in the degree of reduction measurements by iodometric titrations and Na^+ back exchange were as outlined in Part I (*5*). In every instance, 3 g of hydrated sample, in pellet form (1.18–1.70 mm diameter), were reduced in a fixed-bed catalytic reactor (*39*) at a heating rate of 180 K h^{-1}, in a 120 cm^3 min^{-1} stream of purified hydrogen, to 723 ± 2 K, which was then maintained for 18 h. Treatment of the reduced catalyst with ammonia to poison the surface Brønsted acid sites was achieved by passing a 120 cm^3 min^{-1} NH_3 stream through the catalyst bed at 423 ± 1 K for a period of 15 min. The hydrogen flow was then reintroduced and the sample was flushed for 6 h at 473 ± 1 K and heated at 50 K h^{-1} in a 120 cm^3 min^{-1} flow of hydrogen to 723 ± 2 K, which was again maintained for an additional 24 h. Surface acidity was also neutralized by passing a steady 5 cm^3 h^{-1} flow of pyridine or quinoline via a precision motor driven syringe (described in detail in Ref. (*39*)) through the activated catalyst bed at 423 ± 1 K for 30 min, flushing and re-reducing in hydrogen as before. In addition, zeolite samples in the form of thin wafers (surface area 1.3 cm^2) were activated in a specially constructed infrared cell (*5*, *40*) under a 120 cm^3 min^{-1} stream of purified nitrogen at 723 ± 2 K for 18 h. The discs were then outgassed (at 1.3×10^{-3} N m^{-2}) at 723 ± 2 K for an additional hour and the samples were contacted with 2.6×10^3 N m^{-2} CO at room temperature. X-ray diffraction and infrared spectroscopy were used to monitor sample crystallinity before and after reduction according to the criteria of Flanigen *et al.* (*41*).

RESULTS AND DISCUSSION

The chemical compositions of selected ion-exchanged zeolites are given in Table 1.

TABLE 1

Selected Chemical Compositions[a] of the Nickel-Loaded Zeolites Prepared by Ion Exchange

Zeolite sample	AM^+/ UC[b]	Ni^{2+}/ UC	H^+/ UC	Water content (w/w)
NaY	58.0	—	—	25.1
NiNaY-6.8	53.7	2.0	0.3	25.3
NiNaY-15.8	48.8	4.6	—	26.5
NiNaY-22.8	44.0	6.6	0.8	26.6
NiNaY-27.8	40.9	8.1	0.9	26.8
NiNaY-35.7	36.0	10.4	1.2	27.6
NiNaY-48.8	30.0	14.1	—	28.6
NiNaY-63.1	22.3	18.3	—	29.1
NiNaY-78.6	14.6	22.8	—	29.5
NiNaY-90.1	6.9	26.1	—	30.0
KY	58.0	—	—	22.4
NiKY-8.0	53.3	2.3	—	22.3
NiKY-23.5	44.2	6.8	0.2	23.5
NiKY-35.6	36.9	10.3	0.5	24.8
NiKY-44.7	31.9	13.0	0.1	25.5
NiKY-49.1	29.8	14.2	—	26.4
NiKY-57.5	24.8	16.7	—	27.3
NiKY-62.5	22.3	18.1	—	27.6
NiKY-73.8	16.3	21.4	—	28.0
NiKY-82.0	13.1	23.8	—	28.4
NiKY-86.6	8.4	25.1	—	29.3
LiY	58.0	—	—	27.8
NiLiY-8.8	52.3	2.6	0.5	27.9
NiLiY-21.2	44.6	6.2	1.0	28.2
NiLiY-43.1	32.0	12.4	1.2	28.8
NiLiY-63.7	20.7	18.5	0.3	29.3
NiLiY-80.6	14.2	23.4	—	29.9
RbNaY	40.2[c]	—	—	20.4
NiRbNaY-27.3	24.3	7.9	0.2	23.0
NiRbNaY-35.1	19.8	10.2	—	24.2
NiRbNaY-47.4	15.2	13.7	—	25.9
NiRbNaY-59.1	10.3	17.1	—	27.4
CsNaY	39.8[c]	—	—	7.8
NiCsNaY-31.1	20.7	9.0	—	14.9
NiCsNaY-44.3	13.6	12.8	—	16.6
NiCsNaY-54.8	11.2	15.9	—	19.4
NH_4Y	—	—	58.0	24.3
$NiNH_4Y$-8.5	—	2.5	53.0	24.3
$NiNH_4Y$-20.7	—	6.0	46.0	25.5
$NiNH_4Y$-52.2	—	15.1	27.8	27.6
$NiNH_4Y$-69.1	—	20.1	17.9	28.1

[a] Full details of all the prepared samples are given in Ref. (*40*) or are available from the corresponding author on request.

[b] AM^+ = Li^+, Na^+, K^+, Rb^+, or Cs^+.

[c] Number of Rb^+ or Cs^+/U.C.

The tabulated samples are labeled according to the percentage exchange of the indigenous alkali metal ions; e.g., NiKY-23.5 exhibits a 23.5% exchange of the original potassium content, which corresponds to a nickel cation content of 6.8 Ni^{2+}/UC. The extent of H^+ exchange into the aluminosilicate framework during sample preparation was dependent on the nature of the parent zeolite and increased in the order CsNaY < RbNaY < KY < NaY < LiY. This sequence also represents that of decreasing basicity of the bare alkali metal ions. Complete exchange of Na^+ ions for Li^+, K^+, and NH_4^+ was readily achieved, whereas repeated exchange of Rb^+ and Cs^+ ions at elevated temperatures resulted in a much lower maximum level of exchange. Employing the exchange procedure described previously (*5*), the maximum level of Ni^{2+} exchange of NaY and KY was less than 86%. The framework charge on the parent Y zeolites must therefore be too low to displace the waters of hydration from Ni^{2+} at 373 K with the result that progress from the supercages to the sodalite units is restricted. Complete exchange with Ni^{2+} was achieved by calcining the partially exchanged NiNaY/NiKY in flowing nitrogen (120 cm^3 min^{-1}) at 723 K and contacting the anhydrous zeolite with 0.1 mol dm^{-3} $Ni(NO_3)_2$ solutions at 373 K. It is evident from the data presented in Table 1 that the zeolite water content depends on the number and size of the particular cation present. In agreement with Fraissard *et al.* (*42*) the water content increased markedly with nickel loading due to the preferred octahedral coordination (to six water molecules) of the Ni^{2+} cations in the hydrated unit cell. The number of water molecules per unit cell decreased with increasing cation size and coordination energy, i.e., LiY > NaY > KY > RbNaY > CsNaY. Zeolite crystallinity was maintained after preparation for each of the tabulated samples.

Reduction of the Monometallic Ion-Exchanged NiY Samples

The effect of nickel loading on cation reducibility was studied in the case of NiNaY, NiKY, NiLiY, NiRbNaY, and NiCsNaY. The generation of monovalent Ni^+ ions during the reduction process has been well documented in the literature (*43, 44*). Infrared spectra of adsorbed CO (*5, 40*) and ESR studies (*40*) of a number of reduced catalysts confirmed that hydrogen reduction at 723 K resulted solely in the formation of Ni^0. However, the presence of supported Ni^+ was confirmed for hydrogen treatments in the temperature range 403–573 K; the concentration of supported Ni^+ ions was observed to pass through a maximum in the range 433–473 K (*40*). Percentage Ni^{2+} reduction (to Ni^0) is shown in Fig. 1 as a function of nickel content for the NiNaY and NiKY samples. A trend common to both systems is the decrease in the degree of reduction at higher levels of metal cation exchange, reaching a value of ca. 50% at loadings greater than 18 Ni^{2+}/UC. This lends further credence to the contention that the reduction process is an equilibrium governed by the concentration of surface hydroxyl groups since, on reduction, surface hydroxyls are generated according to

$$Ni^{2+}(ZO^-)_2 + H_2 = Ni^0 + 2ZOH,$$

where 2 surface hydroxyls (Brønsted acid sites) are formed, which then limit the extent

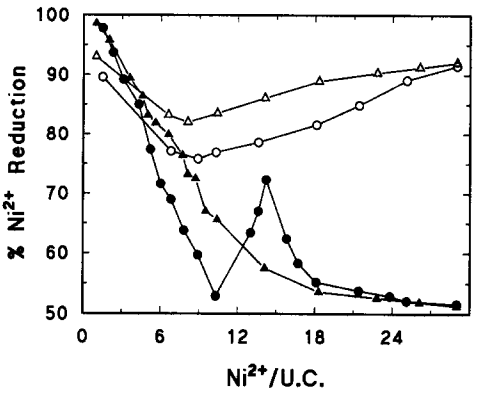

FIG. 1. Percentage Ni^{2+} reduction as a function of nickel loading for the NiNaY (△, NH_3 treated; ▲, untreated) and NiKY (○, NH_3 treated; ●, untreated) systems.

of the reduction process. At low metal loadings, i.e., < 10 Ni^{2+}/UC, the NiKY samples exhibit a significantly lower degree of Ni^{2+} reduction. At this level of exchange, as discussed in Part I (*5*), all the divalent nickel ions are located in the small cages where they are in octahedral coordination with the latice oxygens. When potassium, which has a lower electronegativity than sodium, is present as the indigenous co-cation, the negative charge localized on the zeolite skeleton is greater with the result that the supported Ni^{2+} cations are coordinated more strongly and are therefore more difficult to reduce. However, for nickel loadings greater than ca. 10 Ni^{2+}/UC, NiKY samples exhibit a marked cusp in the reduction profile which, as in the case of the NiNaY system, ultimately reaches a plateau at ca. 50% reduction. We have already shown (*5*) that, at nickel exchanges in excess of 12 Ni^{2+}/UC the additional ions locate in the supercages where they are more readily reduced. At the same time, the large-cage Brønsted acidity generated during reduction is increasing. As discussed in the literature (*45–48*), zeolite acid strength is in direct correlation to electronegativity of the charge-balancing cation. Therefore, when sodium is present as the co-cation, the surface hydroxyl groups exhibit a greater acid strength with the result that the oxidative reaction is promoted to a greater degree. In the case of the NiKY samples, the first four Ni^{2+} cations, which locate in the supercage, are appreciably reduced before zeolite acidity begins to inhibit further reduction. The reduction data obtained from both iodometric titration and Na^+ back exchange techniques (*5*) are compared in Table 2. Although the values obtained from the latter method were lower, particularly for the nickel dilute samples, overall agreement is very good.

TABLE 2

Comparison of Degree of Ni^{2+} Reduction Data Obtained from Iodometric Titration and Atomic Absorption Measurements

Zeolite sample	Percentage Ni^{2+} reduction	
	Iodometric titration	Atomic absorption
NiNaY-6.8	95.7	89.0
NiNaY-17.3	83.1	78.8
NiNaY-22.8	79.3	73.4
NiNaY-29.9	73.7	68.4
NiNaY-35.7	65.4	58.1
NiNaY-48.8	57.2	53.4
NiNaY-63.1	53.1	50.1
NiNaY-78.6	52.1	51.4
NiNaY-90.1	51.9	49.0
NiKY-5.2	97.5	91.1
NiKY-13.0	84.5	76.9
NiKY-23.5	68.9	60.1
NiKY-30.5	60.2	57.7
NiKY-35.6	53.2	50.1
NiKY-49.1	71.8	69.0
NiKY-62.5	54.9	53.2
NiKY-82.0	53.3	52.9
NiKY-86.6	52.7	52.1

To check whether the same argument holds for the lithium-, rubidium-, and caesium-based catalysts, we may examine Fig. 2, where the degree of reduction is again plotted against nickel content. To a large extent, the correlation does hold true. However, as the NiLiY are more acidic than their NiNaY counterparts (*48*), they exhibit a marked decrease in reduction at lower levels of nickel exchange (<6 Ni^{2+}/UC) and the plateau value appears at ca. 40%. Although the degree of reduction of the small cage Ni^{2+} cations is again lower for the more basic NiRbNaY and NiCsNaY samples, the cusp observed in the reduction curve for the NiKY system is not evident. Rather, the level of divalent nickel reduction is maintained at a higher level for the nickel-rich samples. This effect was further developed by examining the reducibility of a series of NiKNaY samples containing a constant amount of nickel (ca. 14 Ni^{2+}/UC) but a varying K^+/Na^+ ratio (Table 3). It can be seen that a progressive increase in the potassium content resulted in an enhancement of Ni^{2+} reducibility, due to the lower surface acidity induced by the presence of K^+ ions

TABLE 3

Degree of Reduction (at 723 K) of Ni^{2+} Cations Supported on a Range of NiKNaY Zeolites of Varying K^+/Na^+ Content

Zeolite sample	Na^+/ UC	K^+/ UC	Ni^{2+}/ UC	Percentage Ni^{2+} reduction
NiNaY-50.0	30.3	—	14.1	54.1
NiKNaY-47.7	23.9	7.0	13.8	53.6
NiKNaY-47.1	15.2	15.8	13.7	57.5
NiKNaY-49.3	10.1	20.3	14.3	60.1
NiKNaY-46.1	7.8	23.7	13.4	61.2
NiKNaY-48.4	3.8	27.1	14.0	64.5
NiKNaY-46.2	—	32.2	13.4	65.9

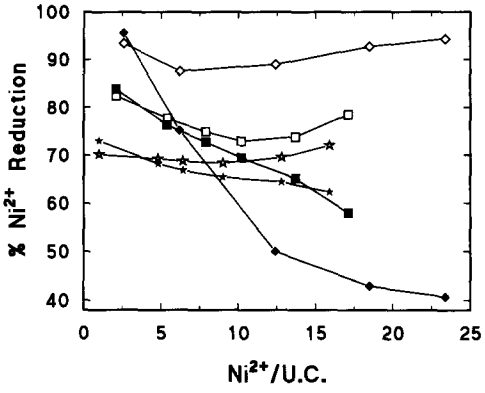

FIG. 2. Percentage Ni^{2+} reduction as a function of nickel loading for the NiLiY (◇, NH_3 treated; ◆, untreated), NiRbNaY (□, NH_3 treated; ■, untreated), and NiCsNaY (☆, NH_3 treated; ★, untreated) systems.

in the zeolite lattice. The degree of reduction of S_I Ni^{2+} cations therefore decreases in the order NiLiY > NiNaY > NiKY > NiRb NaY > NiCsNaY. At higher nickel loadings, where Brønsted acidity begins to play a more important role, this sequence is reversed. In the case of the highly acidic $NiNH_4Y$ samples, Table 4, where the small-cage Ni^{2+} cations should be more easily reduced from a consideration of coordination strengths, the inhibitory effects of the hydroxyl groups prove overwhelming with the result that nickel metal formation is negligible.

To further address the role of surface acidity in inhibiting the reduction process, it was decided to study the effects of neutralizing the acid sites by contacting the activated surface with a base, in this case ammonia, which, because of its size, can diffuse through the zeolite pore structure and "poison" the small-cage Brønsted sites. Indeed, it is well established (*49, 50*) that ammonia adsorbs on zeolitic Brønsted sites to give the protonated adduct. As expected, the initial portion of the reduction vs loading profiles remained unchanged by the ammonia treatment (Figs. 1 and 2). However, the degree of reduction exhibited by the nickel-concentrated zeolites was considerably enhanced (Table 4). As a result of surface acid poisoning, the order of increasing metal ion reduction over the entire range of nickel loadings is now NiCsNaY < NiRbNaY < NiKY < NiNaY < NiLiY. In addition, the higher loaded samples exhibit the greater levels of reduction, indicating that the majority of the supercage Ni^{2+} cations are reduced. From DTG and nitrogen microanalyses, it was found that all of the initially adsorbed ammonia had desorbed from the samples at the final reduction temperature of 723 K. Two desorption peaks were observed at ca. 560 and 660 K, which can be attributed to a deammoniation occurring at

TABLE 4

Comparison of the Relative Effectiveness of Ammonia, Pyridine, and Quinoline as Surface Acid Poisons

Zeolite sample	Percentage Ni^{2+} reduction			
	Ammonia treated	Pyridine treated	Quinoline treated	Untreated
NiNaY-35.7	84.5	77.1	76.2	65.4
NiNaY-78.6	90.3	81.3	79.4	52.1
NiKY-35.6	81.3	72.8	68.5	53.3
NiKY-73.9	88.0	78.7	73.7	53.7
NiLiY-80.6	96.0	83.5	77.0	40.1
NiRbNaY-59.1	78.6	68.0	63.1	57.5
NiCsNaY-54.8	72.1	67.4	65.0	63.3
$NiNH_4Y$-20.7	73.1	57.9	48.1	4.2
$NiNH_4Y$-69.1	72.4	48.4	32.0	1.0

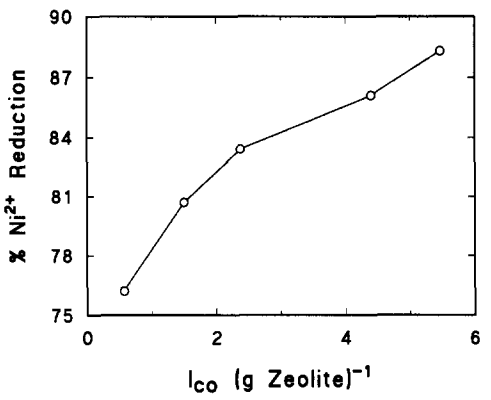

FIG. 3. Relationship between percentage reduction of Ni^{2+} cations supported on NH_3-treated NiKY and the intensity of the infrared bands (2216 and 2200 cm^{-1}) due to CO adsorption on the calcined samples.

two distinct Brønsted sites of different acid strength. Regardless, a considerable portion of the adsorbed ammonia interacted with the zeolite surface, under the slow heating rates employed, over a wide reduction temperature interval. In other words, the surface acid poison was thermally stable in a temperature range where we have previously (*5*) observed Ni^{2+} reduction to occur and can therefore effectively promote additional cation reduction. The data plotted in Fig. 3 illustrate the correlation between the degree of Ni^{2+} reduction for the ammonia-treated samples and the intensity of the infrared bands arising from CO adsorption on calcined NiKY zeolites. It can be seen that nickel reducibility increases with increased CO adsorption and hence with an increase in the number of adsorption sites. From the arguments given in Part I (*5*), this relationship suggests that the degree of reduction depends mainly on the number of reducible Ni^{2+} cations, i.e., CO accessible supercage Ni^{2+} cations. Therefore, on neutralizing zeolite Brønsted acidity, the major influence on the level of Ni^{2+} reduction is the strength of coordination of Ni^{2+} cations to the anhydrous framework.

The ammonia-poisoned $NiNH_4Y$ samples exhibited a significant improvement in Ni^{2+} reduction (Table 4). Nevertheless, the degree of reduction was still considerably lower than that observed for the poisoned NiNaY system, suggesting that not all the acid sites were neutralized during the ammonia treatment. The effectiveness of two other bases, i.e., pyridine and quinoline, to poison the acid sites and so enhance nickel reducibility was also investigated (Table 3). Ammonia proved to be the most effective poison. Pyridine and quinoline, due to their size, are unable to enter the small cages and as a result can only adsorb on the more accessible supercage acid sites. By comparing the relative extent of reduction for the various procedures one can conclude that it is the supercage hydroxyl groups that predominantly retard the reduction process. The higher observed levels of Ni^{2+} reduction for pyridine treatment over that of quinoline may be accounted for by the reported ability of adsorbed pyridine to induce Ni^{2+} ion migration from the small to large cages (*51*) where they are more easily reduced.

It is important to note that, although the degree of reduction decreases as the level of exchange increases in the absence of any form of acid poisoning, the actual mass of nickel metal generated increases with the level of exchange (Fig. 4). In the case of the poisoned samples, where the supercage Brønsted acidity has been effectively neutralized, the mass of supported nickel metal decreases with the increasing basicity of the carrier. Regardless, the ammonia-treated zeolites exhibit the greatest mass of surface metal.

Reduction of the Ion-Exchanged NiCeY Samples

The chemical compositions of the sodium and potassium-based Ni/Ce zeolites are given in Table 5. In these systems the exchange process is further complicated by the fact that, on back exchange of the Ce^{3+} ions, some of the indigenous Ni^{2+} ions are displaced. The interaction between Ni^{2+} and Ce^{3+} ions during calcination and the

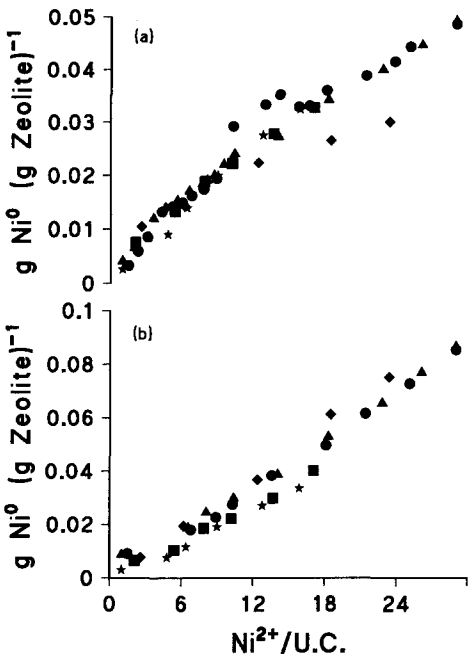

FIG. 4. Plot of the mass of nickel metal generated per gram of zeolite as a function of nickel loading for a range of (a) untreated and (b) NH_3-treated Y zeolites: NiLiY (◆), NiNaY (▲), NiKY (●), NiRbNaY (■), and NiCsNaY (★).

nature of the final cation distribution within the zeolite framework was investigated by a Cs^+ back-exchange procedure described in Part I (*5*). The anhydrous zeolite was treated with a 1 mol dm^{-3} aqueous CsCl solution, the assumption being that the Cs^+ ions exchange with the available large cage Ni^{2+} cations but, because of their size, are unable to remove the metal ions located in the small cages. The number of Ni^{2+} cations remaining in the small cages was then determined by atomic absorption. The accuracy of these measurements is dependent on the absence of Ni^{2+} migration to the small cages during the back-exchange step. Repeated exchange of the rehydrated CsCl-treated samples with 1 mol dm^{-3} $NaNO_3$ solutions to remove the small-cage Ni^{2+} ions revealed that the number of small-cage Ni^{2+} ions inferred from Cs^+ back exchange were in excellent agreement (to within ±2%) with the number of metal cations eluted during the $NaNO_3$ treatment. In the case of CeNaY and CeKY, the Ce^{3+} ions originally located in the supercages in the hydrated samples migrate to the less accessible small cages at elevated temperatures (Fig. 5). It is of interest to note that the migration of Ce^{3+} ions into the small cages becomes constant at ca. 11 Ce^{3+}/UC in the case of CeNaY and ca. 10 Ce^{3+}/UC for CeKY at 473 K. The sodium-exchange capacities, defined in Part I (*5*), i.e., 36.1% for CeNaY-68.0 and 43.4% for CeKY-74.2, indicate an irreversible Ce^{3+} migration from the supercages to the small cages. The Cs^+ back-exchange data for the two component Ni/Ce system are illustrated in Fig. 6. There is a direct competition between the two cations for the energetically favorable small-cage sites. The number of $S_I + S_{I'}$ Ni^{2+} cations dropped from ca. 12 to ca. 7 Ni^{2+}/UC in the presence of Ce^{3+}. From DTG measurements, it was found that cerium ions are stripped of their water sheath at a temperature (444 K) lower than that of the supported nickel ions (456 K). Therefore, during heat treatment, the Ce^{3+} ions are first to gain access to the

TABLE 5

Effect of Ce^{3+} Exchange on the Reduction of Ni^{2+} Ions Supported on NaY and KY

Zeolite sample	Ni^{2+}/ UC	Ce^{3+}/ UC	Percentage H_2O (w/w)	Percentage Ni^{2+} reduction	
				NH_3 treated	Untreated
NiNaY-21.8	6.3	—	25.9	82.1	76.4
CeNiNaY-21.6	6.3	2.3	25.9	79.3	55.0
CeNiNaY-21.1	6.1	7.4	25.8	69.2	34.9
CeNiNaY-20.8	6.0	9.9	25.5	58.0	23.1
NiNaY-58.0	16.8	—	27.8	87.8	53.4
CeNiNaY-54.4	15.8	2.4	27.6	86.0	40.9
CeNiNaY-34.9	10.1	7.5	26.9	69.3	25.4
CeNiNaY-24.0	7.0	10.6	26.1	53.1	14.2
NiKY-25.0	7.2	—	23.2	86.7	62.2
CeNiKY-24.8	7.2	1.7	22.9	84.2	48.1
CeNiKY-24.3	7.1	8.2	22.9	73.3	38.4
CeNiKY-23.9	6.9	10.9	22.7	62.9	30.1
NiKY-56.9	16.5	—	27.1	90.8	55.3
CeNiKY-55.2	16.0	2.2	26.7	90.1	47.1
CeNiKY-48.8	14.1	6.9	25.4	79.1	39.3
CeNiKY-35.7	11.4	9.5	25.4	75.1	28.1

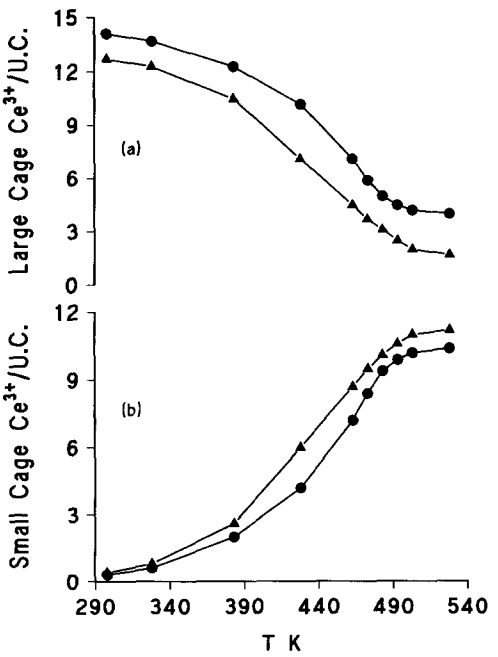

FIG. 5. The variation in the number of (a) large-cage and (b) small-cage Ce^{3+} cations supported on CeNaY-68.0 (▲) and CeKY-74.2 (●) with increasing temperature (in a 120 cm^3 min^{-1} N_2 flow).

small-cage sites, where, by mutual cation repulsion combined with Ce^{3+}/framework interactions, the number of Ni^{2+} ions that can locate at the S_I sites is restricted. The S_I site, although providing optimum coordination possibilities, is therefore only half filled by Ni^{2+} ions due to space restrictions and electrostatic interactions due to the presence of Ce^{3+} ions at S_I, sites. Although the effect of Ce^{3+} ions in displacing Ni^{2+} ions from the small-cage sites has been observed for CeNiNaX (*18, 29*), this phenomenon has not been reported in the case of Ni^{2+}/Ce^{3+}-exchanged Y zeolites.

A number of studies (*19, 29–32*) that show a marked enhancement of Ni^{2+} reduction on exchange of Ce^{3+} into NaX are extant and, from a consideration of cation siting alone, it should follow that CeNiNaY and CeNiKY samples also exhibit greater levels of Ni^{2+} reduction when compared to NiNaY and NiKY. However, the data presented in Table 5 reveal that Ce^{3+} addition actually inhibits cation reduction, an effect that is not fully reversed by treatment with ammonia. Rather, these results agree with the findings of Bager *et al.* (*17*). The presence of Ce^{3+} ions, strongly electron-donating and possessing a high polarizing power, generate protons via the dissociation of the cationic waters of hydration, thereby introducing an additional level of acidity into the zeolite lattice, which will inhibit reduction. The Ce^{3+}/Ni^{2+} ratio and therefore the Ce^{3+} ion concentration determines the reduction properties of the samples studied. The NiKY zeolites retain a higher level of Ni^{2+} reduction on dilution with Ce^{3+} due to the lower overall surface acidity of these samples. The fact that ammonia treatment of the Ni/Ce samples does not bring the level of Ni^{2+} reduction in line with that observed for NiNaY/NiKY suggests the presence of

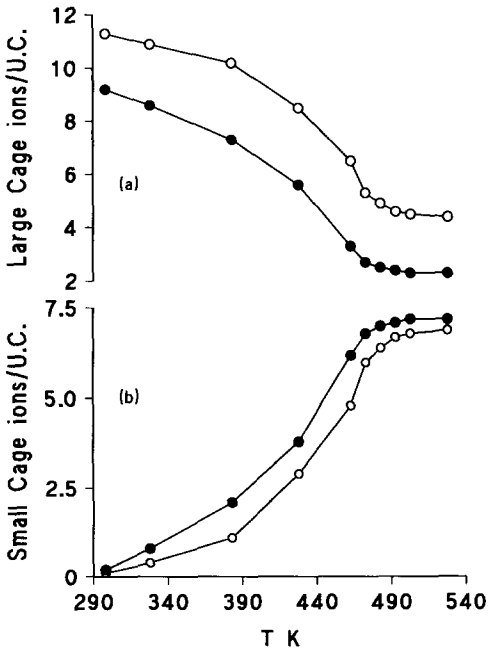

FIG. 6. The variation in the number of (a) large-cage and (b) small-cage Ni^{2+} (○) and Ce^{3+} (●) cations supported on $Ce_{9.5}Ni_{11.4}K_{6.7}Y$ with increasing temperature (in a 120 cm^3 min^{-1} N_2 flow).

TABLE 6

Variation of Ni^{2+} Reduction with Nickel Loading for a Range of Nickel-Impregnated Samples

Impregnated sample	Ni^{2+}/UC	Percentage H_2O (w/w)	Percentage Ni^{2+} reduction
NiO/NaY-0.7[a]	2.0	26.1	96.4
NiO/NaY-6.8	20.3	28.4	83.1
NiO/KY-0.7	2.3	23.6	78.1
NiO/KY-6.5	20.3	25.0	69.9
NiO/LiY-0.8	2.2	27.6	95.9
NiO/LiY-6.8	19.3	28.6	76.0
NiO/RbNaY-0.6	2.3	21.2	73.1
NiO/RbNaY-4.2	15.1	22.9	70.3
NiO/CsNaY-0.7	2.7	10.3	54.2
NiO/CsNaY-3.7	15.2	13.4	68.2
NiO/NH_4Y-0.7	2.1	24.4	10.1
NiO/NH_4Y-6.8	19.9	25.8	6.8
Ni/SiO_2-0.6	—	3.3	100
Ni/SiO_2-2.8	—	3.8	100
Ni/SiO_2-9.7	—	5.2	92.2
Ni/Al_2O_3-0.4	—	3.5	100
Ni/Al_2O_3-2.2	—	4.1	94.1
Ni/Al_2O_3-9.1	—	5.6	63.2

[a] Percentage Ni w/w, based on hydrated unit cell.

a Lewis acid function. Indeed, thermal treatments above 573 K have been shown (*52, 53*) to result in the generation of Lewis acid sites that act as oxidizing centers but remain unaffected by ammonia treatment. It may also be speculated that the presence of Ce^{3+} cations in the small cages interferes with the migration of Ni^{2+}, which has been shown to occur during the reduction process (*5*).

Reduction of the Monometallic Impregnated NiY Samples

The composition of the nickel Y zeolites prepared by impregnation are given in Table 6. Impregnation of the zeolite support with the metal salt was accompanied by a minor degree of ion exchange resulting in an alkali metal ion content slightly lower than expected. The water content of the impregnated samples (Table 6) is noticeably lower than that recorded for the ion-exchanged zeolites in Table 1. This must be due to a crowding effect where the impregnated aluminosilicate cannot accommodate as many water molecules. A comparison of the reducibilities exhibited by three selected ion exchanged and impregnated systems is illustrated in Fig. 7. As can be seen, the impregnated NiO–LiY samples (Fig. 7a) are characterized by a higher degree of divalent nickel reduction than are the Ni^{2+} ion-exchanged samples under identical reduction conditions. This is also the case for the sodium-based Y zeolites and may follow from the general observation that bulk metal oxides are easier to reduce than more finely dispersed metal ions. However, zeolite acidity must also play a considerable role in governing the nature of the metallic phase. Reduction of the impregnated zeolites did not result in any appreciable formation of surface hydroxyls as detected by infrared spectroscopy (*48*). Rather, heat treatment (in flowing hydrogen) of the zeolite-supported

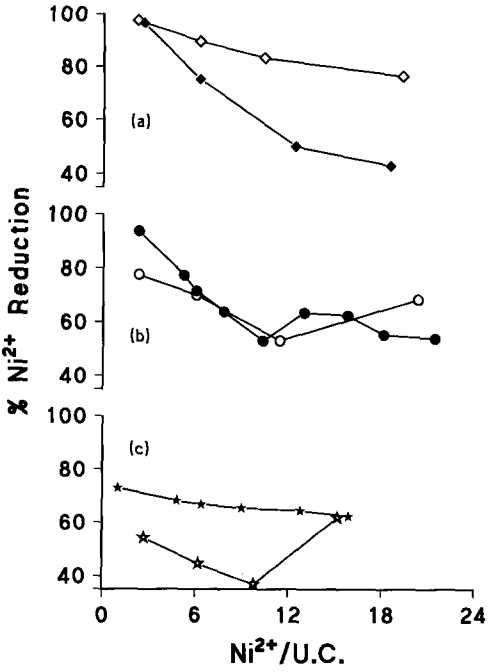

FIG. 7. Percentage Ni^{2+} reduction as a function of nickel loading for (a) NiLiY samples prepared by (◆) ion exchange and (◇) impregnation, (b) NiKY samples prepared by (●) ion exchange and (○) impregnation, and (c) NiCsNaY samples prepared by (★) ion exchange and (☆) impregnation.

nickel salt results in the formation of water and possibly NO_2, NO, or NH_3 as by-products, which are carried away from the zeolite surface in the hydrogen stream without the generation of a Brønsted acid species. The effect of the alkali metal counterions is more pronounced in the case of the impregnated zeolites as they are not displaced to the same extent during sample preparation, resulting in a net higher alkali metal cation concentration. Thus, the inhibitory effect of K^+, Rb^+, and Cs^+ ions, discussed earlier, on the reducibility of small-cage Ni^{2+} cations is greater as shown in Figs. 7b and 7c. Impregnation of the NH_4Y support did not bring about an appreciable increase in Ni^{2+} reduction (Table 6).

As an addendum to our zeolite studies, relevant data on the reduction of nickel ions supported on amorphous silica and alumina carriers are included in Table 6. At metal loadings less than 5% w/w, all the nickel supported on silica was reduced to the metallic state as has been observed by Richardson (*10*). Total Ni^{2+} reduction was also observed for the lower loaded (<4% w/w Ni) Ni/Al_2O_3 samples, but the level of reduction decreased considerably with increasing nickel content. Indeed, the levels of reduction exhibited by the nickel-concentrated alumina samples were similar to those observed for the zeolite-based samples. At a nickel loading of 3% Ni w/w, cation reducibility increases in the order Ni/Y zeolite < Ni/Al_2O_3 < Ni/SiO_2. Furthermore, we have reported elsewhere (*1*) that the metal phase supported on the alumina and silica carriers is in the form of much smaller crystallites. Nevertheless, the possible scope for modification of the metal site within the porous crystalline zeolitic framework is far from exhausted.

CONCLUSIONS

The degree of reduction of Ni^{2+} cations supported on Zeolite Y has been shown to be dependent on the level of nickel exchange and the Brønsted acidity associated with the zeolite. It is proposed that both of these dependencies have a common origin in that the reduction mechanism is viewed as an equilibrium governed by the concentration of acidic surface hydroxyls. The reducibility of Ni^{2+} cations is also influenced by the nature of the counter-ion. At low-exchange levels (<10 Ni^{2+}/UC), the degree of Ni^{2+} reduction decreases with the increasing strength of Ni^{2+} coordination to the zeolite lattice, i.e., NiLiY > NiNaY > NiKY > NiRbNaY > NiCsNaY. At higher nickel loadings, the greater surface acidity associated with the lithium- and sodium-based zeolites is more effective in suppressing the progress of reduction, yielding the sequence of increasing Ni^{2+} reducibility at ca. 16 Ni^{2+}/UC, NiCsNaY > NiRbNaY > NiKY > NiNaY > NiLiY. Hydrogen reduction of a range of $NiNH_4Y$ resulted in negligible Ni^0 formation. Treatment of the reduced samples with ammonia (and to a lesser extent, pyridine and quinoline) followed by a second reduction step generated a greater mass of supported nickel metal due to the poisoning of the surface acid sites. In addition, it has been shown that the incorporation of Ce^{3+} ions into the NiY aluminosilicate framework modifies Ni^{2+} ion location; on complete dehydration, Ce^{3+} ions preferably occupy small-cage sites, forcing some of the Ni^{2+} ions to locate in more accessible positions. Nevertheless, the strong polarizing power associated with the cerium ions, in turn, generates additional surface acidity that inhibits Ni^{2+} reduction. The role of the alkali metal co-cation in determining the extent of metal reduction is more pronounced for the impregnated samples. At low nickel loadings (<4% w/w Ni), percentage reduction decreases in the order Ni/SiO_2 > Ni/Al_2O_3 > Ni/Y zeolite.

REFERENCES

1. Coughlan, B., and Keane, M. A., *Zeolites* **11,** 2 (1991).
2. Coughlan, B., and Keane, M. A., *Catal. Lett.* **5,** 101 (1990).
3. Coughlan, B., and Keane, M. A., *J. Mol. Catal.* **63,** 193 (1990).

4. Coughlan, B., and Keane, M. A., *Catal. Lett.* **5,** 89 (1990).
5. Coughlan, B., and Keane, M. A., *J. Catal.* **123,** 364 (1990).
6. Minchev, Ch., Kanazerev, V., Kosova, L., Penchev, V., Gunsser, W., and Schmidt, F., *in* "Proceedings, 5th International Zeolite Conference" (L. V. C. Rees, Ed.), p. 335, Heyden & Son, London, 1980.
7. Briend-Faure, M., Jeanjean, J., Kermarec, M., and Delafosse, D. *J. Chem. Soc. Faraday Trans. 1* **74,** 1538 (1978).
8. Schubbers, H., Schulz-Ekloff, G., and Wildeboer, H., *Stud. Surf. Sci. Catal.* **12,** 261 (1982).
9. Jacobs, P. A., Nijs, H., Verdonc, J., Derouane, E. G., Gilson, J. P., and Simoens, A. J., *Trans. Faraday Soc. 1* **5,** 1196 (1979).
10. Richardson, J. T., *J. Catal.* **21,** 122 (1971).
11. Suzuki, M., Tsutsumi, K., and Takahashi, H., *Zeolites* **2,** 51 (1982).
12. Penchev, V., Davidova, N., Kanazirev, V., Minchev, H., and Neinska, Y., *Adv. Chem. Ser.* **121,** 461 (1973).
13. Egerton, T. A., and Vickerman, J. C., *J. Chem. Soc. Faraday Trans. 1* **69,** 39 (1973).
14. Davidova, N. P., Valchev, N. V., and Shopov, D. M., *React. Kinet. Catal. Lett.* **16,** 201 (1981).
15. Carru, J. C., Delafosse, D., and Briend-Faure, M., *Stud. Surf. Sci. Catal.* **18,** 337 (1984).
16. Jeanjean, J., Delafosse, D., and Gallezot, P., *J. Phys. Chem.* **83,** 2761 (1979).
17. Bager, K. H., Vogt, F., and Bremer, H., *ACS Symp. Ser.* **40,** 528 (1977).
18. Jeanjean, J., Djemel, S., Guilleux, M. F., and Delafosse, D., *J. Phys. Chem.* **85,** 4145 (1981).
19. Sauvion, G. N., Djemel, S., Tempere, J. F., Guilleux, M. F., and Delafosse, D., *Stud. Surf. Sci. Catal.* **5,** 245 (1980).
20. Tsutsumi, K., Fuji, S., and Takahashi, H., *J. Catal.* **24,** 8 (1972).
21. Kasai, P. H., Bishop, R. J., and McLeod, P., *J. Phys. Chem.* **82,** 279 (1978).
22. Zheng, L., Wang, G., and Bai, X., *Stud. Surf. Sci. Catal.* **28,** 965 (1986).
23. Kermarec, M., Olivier, D., Richard, M., Che, M., and Bozon-Verduraz, F., *J. Phys. Chem.* **86,** 2812 (1982).
24. Halchev, T., Droynov, F., Andreev, A., Davidova, N., and Shopov, D., *Heterog. Catal.* **2,** 361 (1979).
25. Davidova, N. P., Valcheva, M. L., and Shopov, D. M., *Stud. Surf. Sci. Catal.* **18,** 321 (1984).
26. Riekert, L., *Ber. Bunsenges. Phys. Chem.* **73,** 331 (1969).
27. Garbowski, E. D., Mirodatos, C., and Primet, M., *Stud. Surf. Sci. Catal.* **12,** 235 (1982).
28. Exner, D., Jaeger, N. I., Nowak, R., Schulz-Ekloff, G., and Ryder, P., *in* "Proceedings, 6th International Zeolite Conference" (D. Olson, and A. Bisio, Eds.), p. 387, Butterworths, London, 1984.
29. Djemel, S., Guilleux, M. F., Jeanjean, J., Tempere, F., and Delafosse, D., *J. Chem. Soc. Faraday Trans. 1* **78,** 835 (1982).
30. Guilleux, M. F., Delafosse, D., Martin, G. A., and Delmon, J. A., *J. Chem. Soc. Faraday Trans. 1* **75,** 165 (1979).
31. Guilleux, M. F., Kermarec, M., and Delafosse, D., *J. Chem. Soc. Chem. Commun.,* 102 (1977).
32. Briend-Faure, M., Guilleux, M. F., Jeanjean, J., Delafosse, D., Djega Mariadassou, G., and Bureau Tardy, M., *Acta. Phys. Chem., Szeged* **24,** 99 (1978). [In English]
33. Bremer, H., Reschetilowski, W. P., Vogt, F., and Wendlandt, K. P., *Stud. Surf. Sci. Catal.* **18,** 321 (1984).
34. Klyueva, N. V., Valcheva, M. L., Davidova, N. P., Ione, K. G., and Shopov, D. P., *React. Kinet. Catal. Lett.* **17,** 315 (1981).
35. Chien, S. H., Lu, K. L., Huang, H. W., and Hwang, J. M., *Bull. Inst. Chem. Acad. Sin.* **33,** 81 (1986).
36. Marinas, J. M., Caupello, J. P., and Luna, D., *Stud. Surf. Sci. Catal.* **27,** 411 (1986).
37. Richardson, J. T., and Dubus, R. J., *J. Catal.* **54,** 207 (1978).
38. Bartholomew, C. H., and Farrauto, R. J., *J. Catal.* **45,** 41 (1976).
39. Coughlan, B., and Keane, M. A., *Zeolites* **11,** 12 (1991).
40. Keane, M. A., Ph.D. thesis, National University of Ireland, 1988.
41. Flanigen, E. M., Khatami, H., and Szymauski, H. A., *Adv. Chem. Ser.* **101,** 210 (1971).
42. Gedeon, A., Bonardet, J. L., Ito, T., and Fraissard, J., *J. Phys. Chem.* **93,** 2563 (1989).
43. Schoonheydt, R. A., and Roodhooft, D., *J. Phys. Chem.* **90,** 6319 (1986).
44. Michalik, J., Narayana, M., and Kevan, L., *J. Phys. Chem.* **88,** 5236 (1984).
45. Richardson, J. T., *J. Catal.* **11,** 275 (1968).
46. Beran, S., *J. Phys. Chem.* **89,** 5586 (1985).
47. O'Donoghue, E., and Barthomeuf, D., *Zeolites* **6,** 267 (1986).
48. Coughlan, B., and Keane, M. A., *J. Colloid Interface Sci.* **137,** 483 (1990).
49. Earl, W. L., Fritz, P. O., Gibson, A. A. V., and Lunsford, J. H., *J. Phys. Chem.* **91,** 2091 (1987).
50. Teunissen, E. H., van Duisneveldt, F. B., and van Santen, R. A., *J. Phys. Chem.* **96,** 366 (1992).
51. Gallezot, P., and Imelik, B., *J. Phys. Chem.* **77,** 652 (1973).
52. Moscou, L., *ACS Symp. Ser.* **40,** 337 (1977).
53. Hoser, H., Dabrowski, A., and Krzyanowski, S., *ACS Symp. Ser.* **40,** 572 (1977).